JOURNAL OF THERMOPHYSICS AND HEAT TRANSFER
Vol. 24, No. 2, April–June 2010

Flow Rate and Graphite Foam Thermal Management for a Power Amplifier Array

Z. A. Williams*
Miltec Research and Technology, Oxford, Mississippi 38655
and
J. A. Roux†
University of Mississippi, University, Mississippi 38677

DOI: 10.2514/1.46648

Computational fluid dynamics software has been extensively employed in the design of thermal management systems for electronics. There continues to be a need for experimental evaluation of thermal management systems to validate the results of the computational fluid dynamics simulations. This primarily experimental research explores several heat transfer enhancing inserts for a liquid cooled base plate channel design applied to an array of generic power amplifier units. Several different channel insert configurations (both geometric and material type) are investigated as miniheat exchangers using both copper fins and graphite foam. Experimental data were recorded measuring the chip temperatures as a function of volume flow rate. Computational fluid dynamics simulations were also conducted to guide the experimental program. This work has a focus on the volume flow rate impact on the thermal management of a tightly packed array of power amplifiers using liquid cooling.

Introduction

CURRENTLY, there is an emphasis on the importance of thermal design in the area of electronic systems [1]. Thermal design is essential to manufacturing electronic components that will manage dissipated thermal heat and cause it to adequately flow from the heat source to the ambient environment, with the overall thermal management goal being the prevention of system failures and the achievement of the desired electronic system performance and reliability. Rapid increases in performance and reliability demands, as well as a movement toward circuit miniaturization, have led to an increase in chip dissipated heat fluxes [2,3]. This increase in dissipated thermal energy, along with the decrease in overall component size, has heightened the requirement for thermal designs that can manage temperatures within the system below the failure temperature.

There are a variety of methods that are being used to handle the high levels of thermal power that are present in current electronic systems. Forced air-convection cooling of electronics has been popular since the early 90s, mostly due to its simplicity and cost effectiveness [3,4]. Another approach that is applicable is base plate channel cooling; thermal engineers must decide what type of fluid to employ in the cooling channel [5,6]. In many cases, systems that use liquid cooling, although more sophisticated and costly, are necessary to manage the high level of heat power that must be dissipated [7–9]. Heat pipes have been used in high volumes recently by the computer industry in the cooling of processors for notebook computers and may be well suited for designs where space management is a concern [10]. Recently, the use of nanofluids [11] has attracted some investigation with respect to cooling of electronics. Significant work has been done by Dirker et al. [12–16] with the use of solid conductive heat spreaders as a means of effective thermal management.

It is essential, with the many approaches available, that each cooling system be investigated on a case-by-case basis. Computer simulation has become an invaluable tool for significantly improving thermal management for particular applications. Computational fluid dynamics (CFD) software is effectively used by thermal engineers to aid in the design of cooling systems for electronics. The current work uses CFD simulations as a guide for experimental simulations to develop a thermal management system for an array of power amplifier units with the emphasis on the experimental testing. A previous companion study [17] investigated the use of two heat transfer enhancing materials, carbon graphite foam and copper fins, as miniheat exchangers in a base plate cooling channel with air as the cooling fluid. This previous work showed that these cooling channel inserts significantly reduced the power amplifier temperatures by as much as 40°C or more (see Fig. 1). This present work is also a follow-up experimental study to previous work [18,19] to explore cooling mechanisms with water as the cooling fluid with a present emphasis on flow rate impact; the flow rate data contained in this work are unique and have not been included in our previous work [17–19]. For the current study, several different geometric configurations of graphite foam and copper were placed in the cooling channel to act as miniheat exchangers and enhance the convective heat transfer in the channel. The carbon graphite foam used was pyrolytic foam with an open cell structure that yields a large surface area and high porosity, which enhances the convective heat transfer [20,21].

Statement of Problem

The focus of the present work is the thermal management of an array of power amplifier units. The power amplifier unit of interest in the current work consists of an aluminum nitride substrate that is populated with chips and circuitry. The electronics are enclosed by a cover to protect the chips from environmental elements.

Seven chips of varying levels of thermal energy dissipation, one being the power chip, populate each unit. The power chip has a much (orders of magnitude) higher dissipated thermal power than the other six chips and is, therefore, the critical component and the focus of the current study. It is imperative that the temperature of the power chip on each module be maintained below the maximum allowable temperature of 150°C; therefore, electronic failure is assumed to occur at temperatures above 150°C.

In the current investigation, four units are mounted side by side on a copper base plate and will be referred to as a stick. Figure 2 illustrates this with the covers removed from the modules exposing the chips. The base plate has a cooling channel located directly under the units through which water is forced at various flow rates (1.58×10^{-5} m^3/s [0.25 gal/min], 3.15×10^{-5} m^3/s [0.50 gal/min], and

Presented as Paper 4245 at the 41st AIAA Thermophysics Conference, San Antonio, TX, 22–25 June 2009; received 7 August 2009; revision received 28 October 2009; accepted for publication 28 October 2009.

*Engineer.
†Faculty, Mechanical Engineering Department. Associate Fellow AIAA.

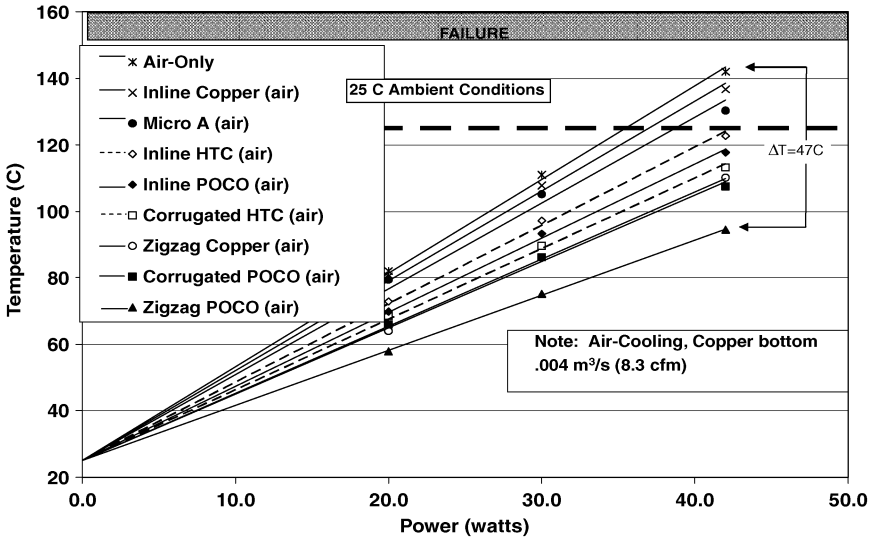

Fig. 1 Air cooling results from previous research [17].

6.31×10^{-5} m^3/s [1.00 gal/min]). Water flowing through the channel removes the heat dissipated by the power chips through forced convection. The sticks previously described are mounted in a cabinet to isolate them from the environment. As depicted in Fig. 3, there are four sticks mounted in the cabinet with each stick containing four units; thus, the overall array contains 16 (4×4) power amplifier units. The electrical performance criteria require that a packing tightness of 0.020 m must be maintained to ensure proper electrical operation; this is the distance from the bottom of one base plate to the bottom of the next adjacent base plate with an air gap between sticks of 0.009 m.

Here, several materials were investigated to determine their capability to enhance the heat transfer inside the cooling channel of the base plate. These materials were inserted into the cooling channel directly under the power chip units. Three geometric configurations (inline, corrugated, and zigzag) of two types (Poco medium thermal conductivity foam and Poco high thermal conductivity [HTC] foam) of graphite foam and two configurations of copper fins (inline and zigzag) were investigated.

An improved process of graphitizing carbon foam was developed at Oak Ridge National Laboratories (ORNL), and this process has been licensed to Poco Graphite, Inc. [20]. Graphite foam was installed in the water-cooled base plate in three different configurations: inline, corrugated, and zigzag. Figure 4 depicts exaggerated sketches of each foam geometric configuration. The arrows indicate the path of the fluid. The inline and corrugated configurations were designed based on specifications made by Klett at ORNL. [‡] The proposed advantage to using these foams is that the porosity of the foam provides an increased amount of interior surface area to convectively interact with the fluid in the cooling channel.

Experimental Procedure

CFD simulations were conducted using IcePak®, a CFD software package from Fluent Inc., before the fabrication of any base plates to simulate and guide the experimental setup. These CFD simulations revealed that of the seven chips (see Fig. 2) that populate the power amplifier unit, only the power chip exhibits a significant impact on the unit temperature; thus, for the experimental testing only the power amplifier chip was simulated. CFD simulations also indicated that the chip temperatures of the units on one stick are essentially independent of the chip temperatures on adjacent sticks. This allowed for only one stick to be simulated experimentally. However, to maintain the integrity of the flowfield and to preserve the packing tightness of 0.020 m mentioned earlier, the other sticks were replaced with dummy sticks made of Plexiglas®. These modifications facilitated faster experimental hardware buildup and improved the experimental quality.

Figure 5 is a photograph of the base plate with the environmental cover removed exposing the power chips. A $100\Omega(\pm 0.5\Omega)$ chip resistor manufactured by American Technical Ceramics (LR13737T0100J) was employed to simulate the power chip. The dimensions and material architecture of this resistor (9.40 mm$\times$ 9.40 mm $\times$ 1.87 mm) are similar to that expected for a realistic power amplifier chip. The details of the three-layer chip architecture are contained in Table 1.

The base plate was fabricated in two sections to facilitate easy access to the cooling channel. The primary section of the base plate, referred to as the top, is 4.76 mm (0.188 in) thick and has the electronic chips mounted to one side and the cooling channel machined in the other side; it is fabricated from alloy 110 copper [$k = 391$ W/(m C), thermal conductivity]. Details of the dimensions for the base plate and cooling channel are contained in Fig. 6. The cooling channel within the base plate is 32.6 mm wide and has a height of 3 mm. The other part of the base plate, referred to as the bottom, is 1.59 mm (0.0625 in) thick. Experimental tests were conducted with a bottom section made of Plexiglas® so that the flow inside of the cooling channel could be monitored.

The three different geometrical configurations (inline, corrugated, and zigzag) of graphite foam that were investigated are illustrated in Fig. 7. For each of these geometric configurations, Poco foam and Poco HTC foam types were tested. The Poco foam has a thermal conductivity of 135 W/(m C) in the downward direction and a total porosity of 75%. The Poco HTC foam has a thermal conductivity of 245 W/(m C) in the downward direction and a total porosity of

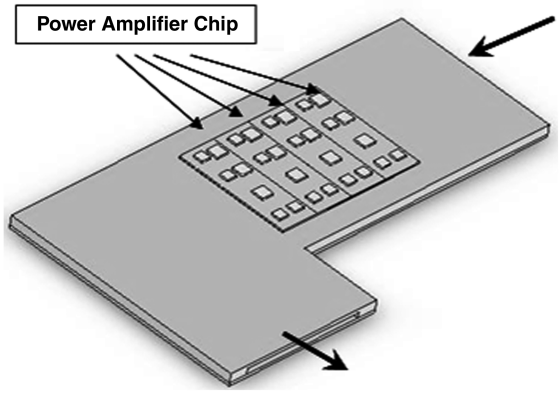

Fig. 2 Water-cooled base plate (top) with substrates and chips.

[‡]Private communication with J. Klett, September 2004.

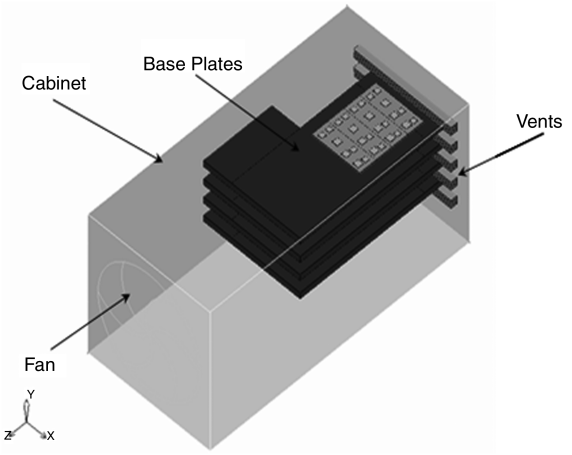

Fig. 3 IcePak® sketch of water-cooled design.

61%[§]. Both a high thermal conductivity and a high porosity are desirable, but these two properties (to some degree) counteract one another. A high thermal conductivity draws heat from the base plate into the cooling channel and allows high heat transfer to occur at a lower overall temperature difference. A high porosity allows more interior surface area for convectively drawing the heat from the foam and into the cooling fluid. For the zigzag and inline configurations, experiments were conducted in which the fins were also made of copper instead of graphite foam for comparison purposes. All of the configurations have a fin height of 3 mm. The dimensions of the fins for the inline and corrugated configurations were based on directives from ORNL[§]. Table 2 contains the dimensional specifications for the various cooling configurations. The fins for the inline configuration have a thickness of 1.6 mm and are separated by a gap of 2.4 mm. The corrugated configuration has a fin thickness of 3.2 mm with a gap between fins of 1.6 mm[§]. The fins for the zigzag configuration have a thickness of 3.7 mm separated by a gap of 6.4 mm; for the zigzag cooling configuration a fin is placed directly beneath where a chip resistor is mounted on the opposite side of the base plate. Also, based on CFD predictions, the zigzag fins were made to a length of 80% (26 mm) of the cooling channel width. For all configurations, as recommended by Klett and Conway [20], the material was held in place with a silver loaded epoxy (DM6030HK) obtained from DIEMAT®. This epoxy has a very high thermal conductivity (60 W/(m C)) as compared with other epoxies and adhesives.

Figure 8 shows the cooling channel with a sample of the copper zigzag fins installed. Figure 9 portrays the experimental apparatus for the water-cooled base plate incorporating a pump, expansion tank, and heat exchanger. The water travels through a manifold before entering and after exiting the base plate. Ten sheets of nylon screen with a mesh size of 1.8 mm and a wire diameter of 0.25 mm were inserted into the inlet manifold to ensure a uniform flowfield inside the cooling channel. The pump, which was manufactured by Little Giant Company (P/N: 977409), was used to circulate the water through the base plate cooling channel. The heat exchanger, manufactured by Lytron™ (P/N: M05-050SB1), was implemented to remove the heat from the cooling fluid before recirculating the water. An Omega acrylic rotameter (P/N: FL7301) was used to monitor the volume flow rate through the cooling channel; this rotameter has an accuracy of 6% full scale (FS) and a repeatability of 1% FS.

Power for the chips was supplied by two variable DC power supplies. Two digital multimeters were used to accurately monitor the voltage (Fluke 37) and current (Fluke 8010A) being supplied to the chips. The temperature at the top of each power chip was measured with type-*J* thermocouples (±0.5 C) and recorded using a data acquisition system (HP VEE). Experiments were con-

[§]Data available online at http://www.poco.com [retrieved Oct. 2006].

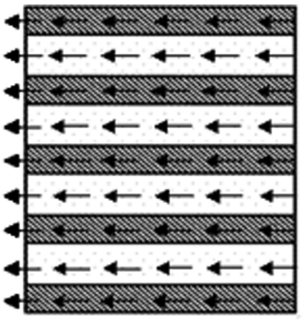

a) Inline configuration

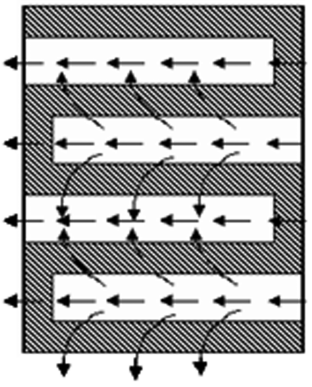

b) Corrugated configuration

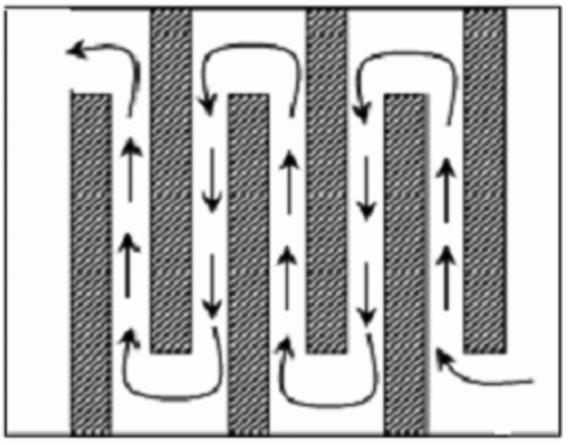

c) Zigzag configuration

Fig. 4 Graphite foam configurations.

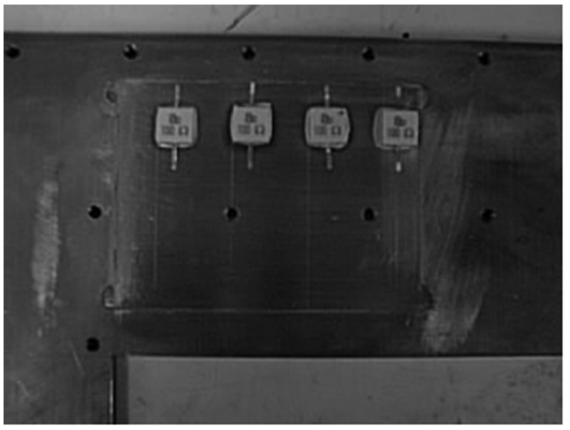

Fig. 5 Base plate with chip resistors.

Table 1 Material properties of chip resistor used to simulate power amplifier chip

Chip layer	Material	Thickness, mm	k, W/(m C)	Density, kg/m^3	Specific heat, J/(kg C)
Substrate	AlNi	1.02	170	3970	910
Resistive element	Tantalum	0.55	57.5	16650	153
Cover	Alumina	0.30	27	3260	740

[a]Chip base area is 9.4 mm × 9.4 mm.

ducted with dissipated thermal power levels of 20 (±0.13 W), 30 (±0.18 W), and 42 W (±0.25 W) input into each power chip. Having described the experimental setup and procedure, the results from this study will be presented in the next section.

Results

The experimental data shown in Figs. 10–21 represent the steady-state temperatures of the power chips at the different levels of dissipated thermal power and volume flow rates of water in the cooling channel both with and without a variety of inserts (both geometric and material type) into the cooling channel to enhance the heat transfer and, hence, reduce the power chip temperatures. Data are expressed in terms of measured power chip temperature as a function of measured dissipated thermal power with flow rate as a parameter. All the experimental data illustrate a linear behavior; this can be beneficial in predicting power chip temperatures at other power levels and at other ambient temperature environments. This linear trend also agrees with the CFD simulations as will be shown. Three base plates were fabricated to expedite the experimental process. A different base plate was used for each geometric configuration (inline, corrugated, and zigzag). Before inserting any graphite foam or copper material into the cooling channel, data were obtained with water-only cooling to establish a baseline against which each of the enhancement inserts could be compared. Clearly, it is desired that any insert of graphite foam or copper fins would reduce the power chip temperatures below the water-only baseline temperature values. All data were obtained at an ambient temperature T_∞ of 25°C.

The water-only (no inserts) cooling data at three different flow rates are shown in Figs. 10–12. The data are seen to be quite linear;

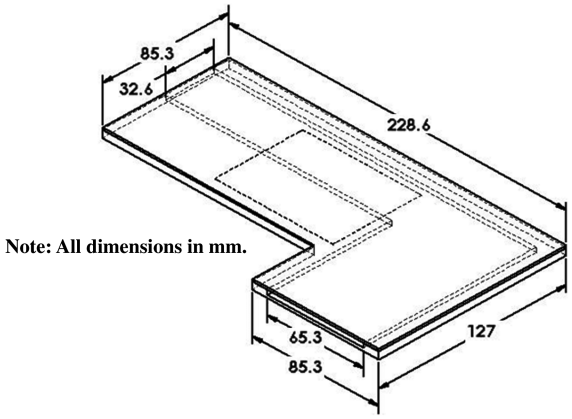

Fig. 6 Water-cooled base plate sketch.

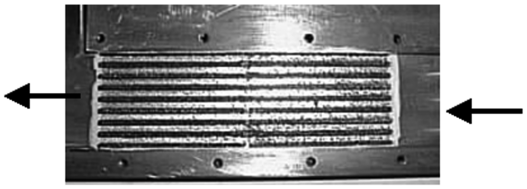

a) Inline configuration

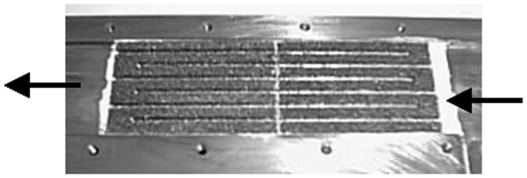

b) Corrugated configuration

c) Zigzag configuration

Fig. 7 Graphite foam configurations in cooling channel.

Table 2 Graphite foam and copper fin configurations specifications

Configuration	Fin thickness, mm	Spacing, mm	Fin length, mm	Number of fins
Inline	1.6	2.4	97	9
Corrugated	3.2	1.6	97	7
Zigzag	3.7	6.4	26	9

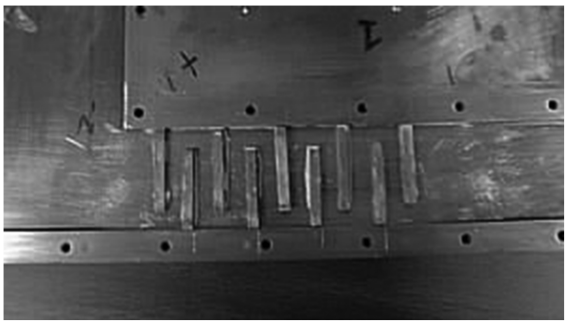

Fig. 8 Stick with copper zigzag fins in cooling channel.

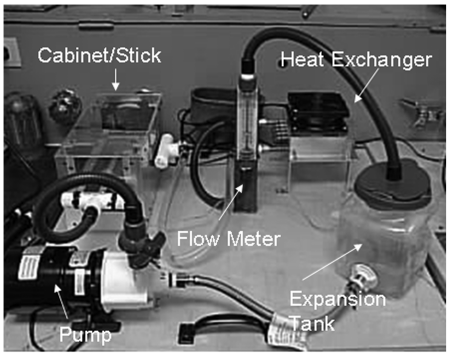

Fig. 9 Water cooling flow circuit setup.

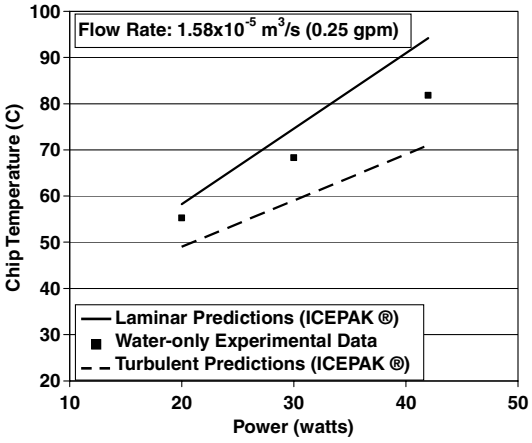

Fig. 10 Comparison of water-only experimental data to laminar and turbulent Icepak® predictions for 1.58×10^{-5} m^3/s flow rate and $T_\infty = 25$°C.

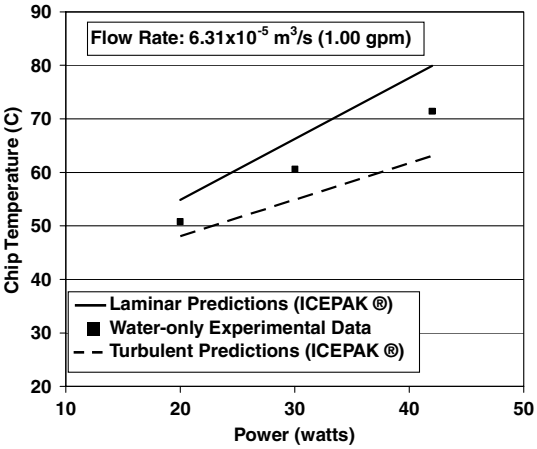

Fig. 12 Comparison of water-only experimental data to laminar and turbulent Icepak® predictions for 6.31×10^{-5} m^3/s flow rate and $T_\infty = 25$°C.

the higher-volume flow rates through the closed-loop cooling system are seen to yield lower power chip temperatures as expected. There is about a 10°C at 42 W chip temperature decrease (Fig. 10 data compared with Fig. 12 data) affected by the increased flow rate for the water-only cooling scheme. Figures 10–12 also illustrate a comparison of the IcePak® predictions for fully laminar or fully turbulent flow as compared with the experimental data. It is seen that the data and predictions agree qualitatively (linear variation) and it appears that the flow is probably transitional in nature because the data for all three (Figs. 10–12) flow rates lie between the fully laminar and fully turbulent flow regime predictions. The qualitative agreement between the CFD predictions and the experimental data for all three flow rates with the inline and zigzag copper fins configurations were similar to that shown in Figs. 10–12 (water-only). That is, the experimental data for the inline and zigzag copper fin configurations were between the fully laminar and fully turbulent CFD predictions, which again implies transitional flow. The IcePak® CFD model employed about 500 K computational nodes to model the entire cabinet interior geometry depicted in Fig. 3. The grid inside the cooling channel was successively made finer until the chip temperature results were independent of grid size. The k-ε turbulence model was employed for the turbulent flow computational results shown in Figs. 10–12. IcePak® employs the finite volume method to solve the entire domain of this conjugate heat transfer problem defined geometrically in Fig. 3.

Figures 13–15 depict, respectively, the flow rate effect for the three geometric configurations with the Poco HTC graphite foam material. Figure 13 illustrates the impact of flow rate on the Poco HTC foam with the inline geometry; the impact of flow rate is seen to yield about an additional 7°C at 42 W of thermal management cooling enhancement. All three flow rates produce substantially lower power chip temperatures as compared with the counterpart water-only data in Figs. 10–12. Shown in Fig. 14 is the influence of flow rate for the Poco HTC corrugated configuration. The flow rate is seen to produce at 42 W about a 6°C reduction in the power chip temperature; all chip temperatures at 42 W are significantly lower than the water-only data shown earlier. Figure 15 demonstrates the flow rate effect for the Poco HTC zigzag geometry; the flow resistance for this geometry was such that the high flow rate could not be achieved with the water pump employed in this experimental test system. There was only about a 1°C enhancement between the low and middle flow rate values; hence, there would be no need to increase the flow rate beyond the low flow rate value.

Figures 16–18 illustrate the flow rate impact for the three geometric configurations for the Poco (higher porosity, lower thermal conductivity) graphite foam. Seen in Fig. 16 is an overall lowering in chip temperatures at 42 W of about 7°C as the flow rate is increased. The increased flow rate increases the convective interaction between the water and the Poco foam, which causes the 7°C improvement in thermal management performance. Figure 17 illustrates that there is only about a 4°C reduction in power chip temperature at 42 W for the corrugated Poco graphite foam configuration. The increased interaction of the water and foam with the higher flow rate does not yield much of an improvement over the low flow rate thermal performance. Finally, Fig. 18 depicts that the zigzag geometric configuration performance for the Poco foam yielded only about a 2°C reduction in chip temperature; the resistance to the flow for this configuration was such that the pump used in the test system could not achieve the high flow rate value.

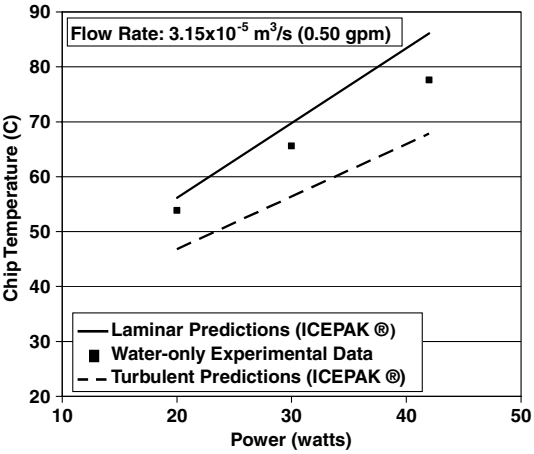

Fig. 11 Comparison of water-only experimental data to laminar and turbulent Icepak® predictions for 3.15×10^{-5} m/s flow rate and $T_\infty = 25$°C[18].

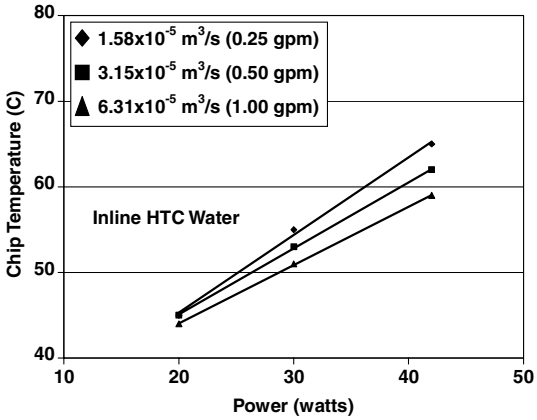

Fig. 13 Flow rate comparison for inline Poco HTC graphite foam water cooling, $T_\infty = 25$°C.

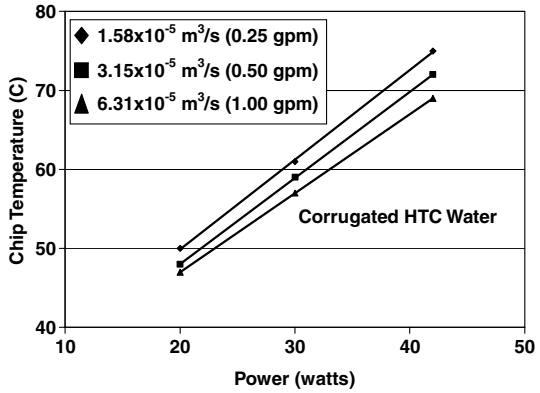

Fig. 14 Flow rate comparison for corrugated Poco HTC graphite foam water cooling, $T_\infty = 25°C$.

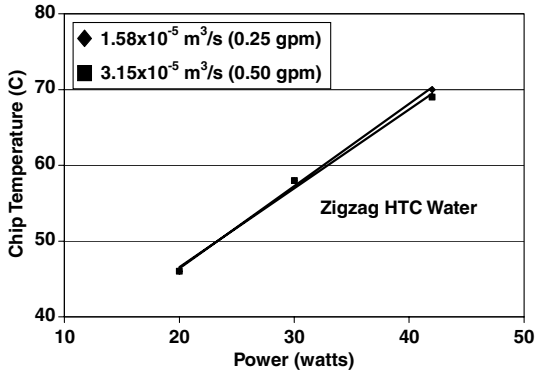

Fig. 15 Flow rate comparison for zigzag Poco HTC graphite foam water cooling, $T_\infty = 25°C$.

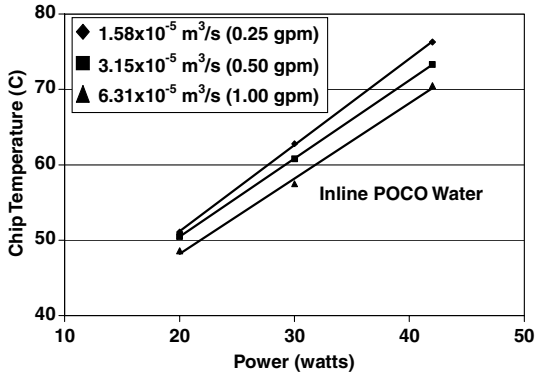

Fig. 16 Flow rate comparison for inline Poco graphite foam water cooling, $T_\infty = 25°C$.

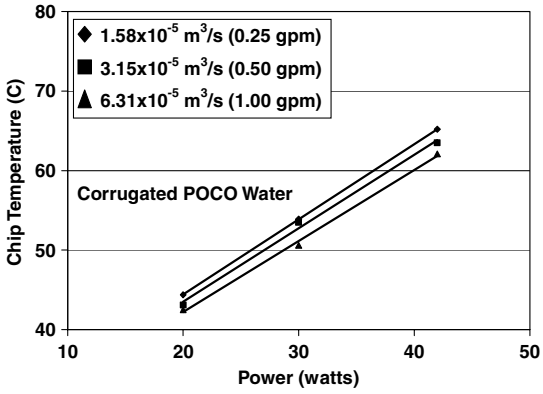

Fig. 17 Flow rate comparison for corrugated Poco graphite foam water cooling, $T_\infty = 25°C$.

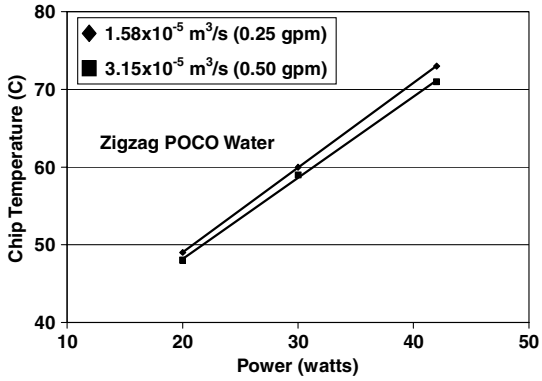

Fig. 18 Flow rate comparison for zigzag Poco graphite foam water cooling, $T_\infty = 25°C$.

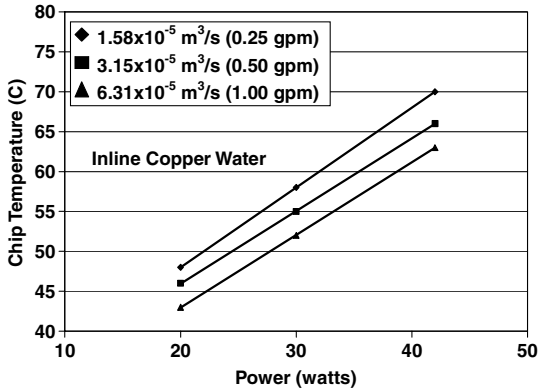

Fig. 19 Flow rate comparison for inline copper water cooling, $T_\infty = 25°C$.

Figures 19 and 20 correspond to the inline and zigzag geometries for the pure copper fin material; the corrugated configuration would totally block the cooling channel of all flow and obviously was not tested. The pure copper fins were investigated because they have a very high thermal conductivity but zero porosity. This was studied for comparison with the Poco and Poco HTC foams that have lower thermal conductivities than pure copper; however, the foams are also porous, which permits convective interaction with the large internal pore surface area to enhance heat transfer. The inline copper fin geometry showed a somewhat stronger (7°C) decrease with flow rate than the zigzag geometry (~4°C). Both pure copper geometric configurations showed a substantial improvement over the water-only data (Figs. 10–12).

Shown in Fig. 21 is the overall comparison of all of the geometric configurations and foams tested. Three of these (inline Poco HTC foam, zigzag copper, corrugated Poco foam) all showed about the same best performance (at 42 W) by reducing the chip temperature by about 16°C for the middle flow rate; the low flow rate (not shown) also showed a chip temperature reduction of about 16°C. Some of the temperature differences among the different configurations in Fig. 21 are relatively small, but these temperature differences are significant relative to the temperature uncertainty given earlier.

Inline Configuration

The results for the inline geometric configuration for both the Poco foam and the HTC Poco foam as well as the inline copper configuration are shown in Fig. 21. All inline configurations performed better than the water-only cooling, with the higher thermal conductivity foam (Poco HTC) yielding the best improvement. The

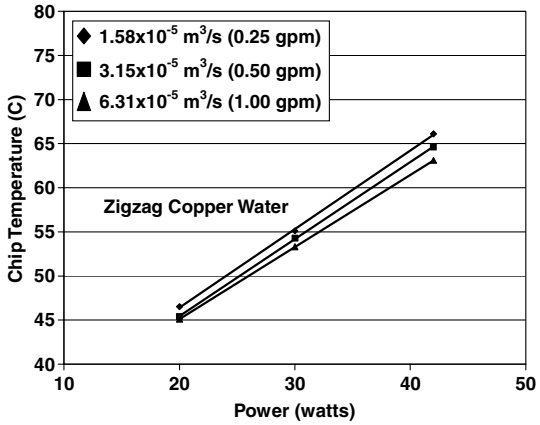

Fig. 20 Flow rate comparison for zigzag copper water cooling, $T_\infty = 25°C$.

water does not appear to interact strongly with the foam pores to access the large interior surface area for heat transfer, but rather the higher thermal conductivity and lower porosity foam (Poco HTC) is better. The Poco foam has a higher porosity than the Poco HTC, but the Poco has a lower thermal conductivity than the Poco HTC foam. For the inline configuration it appears that foam thermal conductivity is more important than porosity, which implies the water probably does not penetrate deeply into the foams. From Fig. 21 both foams performed better than the water-only cooling; the Poco HTC yields chip temperatures about 16°C lower (at 42 W) than the water-only cooling chip temperatures. The inline pure copper fin configuration performed thermally better than the lower thermal conductivity Poco foam but did not function as well as the higher thermal conductivity HTC Poco foam; thus, the interaction of the HTC Poco interior pore surface is seen to result in better performance than just the very high thermal conductivity copper inline fins.

Corrugated Configuration

The power chip temperatures for the corrugated configuration as a function of foam type are illustrated in Fig. 21. With the corrugated configuration the water is made to pass through the foam along the legs (fins) of the corrugated geometry. In this geometric situation the higher (Poco) porosity foam yields the best performance. Because the water is forced to pass through the foam, the higher porosity foam, and thus, higher surface area for heat transfer, more effectively draws heat from the base plate and convects the heat from the high internal pore area into the cooling fluid. In the corrugated configuration, the Poco foam performance is best and lowered the chip temperature by about 16°C (at 42 W) as compared with water-only cooling. The order of performance for the corrugated configuration is the same here as for the air-cooling [12] performance.

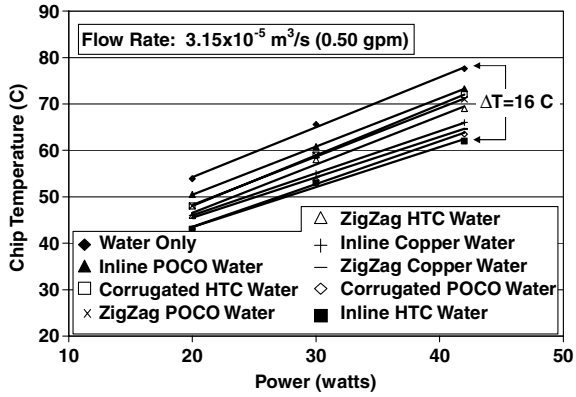

Fig. 21 Summary for water-cooling configurations at a flow rate of 3.15×10^{-5} m/s, $T_\infty = 25°C$ [18].

Zigzag Configuration

Results for the zigzag geometric arrangement are shown in Fig. 21 with copper zigzag fins also being tested. The results in Fig. 21 indicate that, for the zigzag configuration, the performance improves as the thermal conductivity of the insert increases; the copper zigzag fins yielded the best performance. It seems that the viscous water prefers to go around the zigzag pattern and that the water does not penetrate much into or through the foams. The heat transfer appears to occur at the outside wall of the zigzag foam fins and no strong convective interaction occurs with the interior pore area of the foam. Hence, the material with the highest thermal conductivity demonstrated the best performance. The copper zigzag fins show about a 14°C lower chip temperature performance as compared with water-only cooling. Air-cooling [17] results showed the reverse order of performance to that shown for the zigzag configurations in Fig. 21. It seems that the higher-viscosity water is not able to penetrate very well into the foams to take advantage of the high internal pore area for heat transfer enhancement purposes, but that most of the heat transfer occurs away from the interior pore area of the foams and occurs on the outside (planar) area of the foams.

The goal was to maintain temperatures below the failure temperature of 150°C for a thermal dissipated power level of 42 W, even at severe ambient desert temperatures (50°C). IcePak® simulations predict that the power amplifier temperatures will shift (increase or decrease) by the amount of difference in the ambient temperature from 25°C. Assuming the CFD predictions are accurate, all of the configurations experimentally tested would yield power chip temperatures below 150°C if the lines in all of the figures were shifted upward by 25°C to simulate a desert ambient temperature of 50°C. However, the better performing cooling channel inserts would permit even much higher heat dissipation levels in the power chips before reaching the failure temperature of 150°C even at desert conditions. For example, using the present linear experimental data, the inline Poco HTC from Fig. 21 would allow (project) a thermal heat dissipation of about 125 W before reaching the failure temperature of 150 C at desert conditions ($T_\infty = 50°C$).

Conclusions

The results obtained in this work show that all of the cooling configurations experimentally evaluated did demonstrate some significant improvement over water-only cooling (no inserts). In general, all the inserts proved to have strong potential as miniheat exchangers. The best overall performance reduced the chip temperatures at 42 W of heat dissipation by about a ΔT of 16°C as compared with the water-only cooling; there was a ΔT of about 47°C [17] at 42 W for the air-cooling best performance with insert as compared with the air-only cooling. However, the chip temperatures were significantly lower (about 62°C) for the water cooling with insert as compared with the air cooling (about 95°C) with insert at 42 W of thermal dissipation. This was due to the much higher effective convective heat transfer coefficient achieved by the water cooling cases.

Results showed that increasing the flow rate in the cooling channel resulted in lower power chip temperatures; however, the flow rate effect was most significant for the water-only cooling case. It is hoped that the experimental data presented here will help other researchers and designers in achieving thermal management solutions in tight-packing situations of electronic components.

References

[1] Azar, K., "Cooling Technology Options, Part 1," *Electronics Cooling*, Vol. 9, No. 3, 2003, pp. 10–14.

[2] Yeh, L. T., and Chu, R. C., *Thermal Management of Microelectronic Equipment*, American Society of Mechanical Engineers, Fairfield, NJ, 2002.

[3] Chu, R. C., "The Challenges of Electronic Cooling: Past, Current, and Future," *Journal of Electronic Packaging*, Vol. 126, No. 4, 2004, pp. 491–500. doi:10.1115/1.1839594

[4] Bar-Cohen, A., "Thermal Design and Control," *Physical Architecture*

of VLSI Systems, edited by R. J. Hannemann, A. D. Kraus, and M. Pecht, Wiley, New York, 1994, Chap. 9.

[5] Incropera, F. P., *Liquid Cooling of Electronic Devices by Single-Phase Convection*, Wiley, New York, 1999.

[6] Muwanga, R., and Hassan, I., "Flow and Heat Transfer in a Cross-Linked Silicon Microchannel Heat Sink," *Journal of Thermophysics and Heat Transfer*, Vol. 22, No. 3, 2008, pp. 333–341. doi:10.2514/1.33952

[7] Yamamoto, H., Udagawa, H. Y., and Suzuki, M., "Cooling System for FACOM M-780 Large Scale Computer," *Cooling Technology for Electronic Equipment*, edited by W. Aung, Hemisphere, New York, 1988, pp. 701–730.

[8] Kishimoto, T., and Ohsaki, T., "VLSI Packaging Technique Using Liquid-Cooled Channels," *IEEE Transactions on Components, Hybrids and Manufacturing Technology*, Vol. 9, No. 4, 1986, pp. 328–335. doi:10.1109/TCHMT.1986.1136661

[9] Marotta, E. E., Ellsworth, M., and Mazzuca, S., "Thermal Performance of Silicon-Die/Water-Cooled Heat-Sink Assembly: Experimental Investigation," *Journal of Thermophysics and Heat Transfer*, Vol. 18, No. 2, 2004, pp. 193–202. doi:10.2514/1.10175

[10] Garner, S. D., "Heat Pipes for Electronics Cooling Applications," *Electronics Cooling*, Vol. 2, No. 3, 1996.

[11] Bahrami, M., Yovanovich, M., and Culham, J., "Assessment of Relevant Physical Phenomena Controlling Thermal Performance of Nanofluids," *Journal of Thermophysics and Heat Transfer*, Vol. 21, No. 4, 2007, pp. 673–680. doi:10.2514/1.28058

[12] Dirker, J., Liu, W., Van Wyk, J. D., Meyer, J. P., and Malan, A. G., "Embedded Solid State Heat Extraction in Integrated Power Electronic Modules," *IEEE Transactions on Power Electronics*, Vol. 20, No. 3, 2005, pp. 694–703. doi:10.1109/TPEL.2005.846532

[13] Dirker, J., Van Wyk, J. D., and Meyer, J. P., "Cooling of Power Electronics by Embedded Solids," *ASME Journal of Electronic Packaging*, Vol. 128, No. 4, 2006, pp. 388–397. doi:10.1115/1.2351903

[14] Dirker, J., Malan, A. G., and Meyer, J. P., "Thermal Characterization of Rectangular Cooling Shapes in Solids," *International Journal of Numerical Methods for Heat and Fluid Flow*, Vol. 17, No. 4, 2007, pp. 361–383. doi:10.1108/09615530710739158

[15] Dirker, J., and Meyer, J. P., "Heat Removal from Power Electronics in Two Direction Sets Using Embedded Solid State Cooling Layers: A Proposed Non-Numerical Calculation Method," *Heat Transfer Engineering*, Vol. 30, No. 6, 2009, pp. 452–465. doi:10.1080/01457630802528745

[16] Dirker, J., and Meyer, J. P., "Thermal Characterization of Embedded Heat Spreading Layers in Rectangular Heat-Generating Electronic Modules," *International Journal of Heat and Mass Transfer*, Vol. 52, Nos. 5–6, 2009, pp. 1374–1384. doi:10.1016/j.ijheatmasstransfer.2007.10.045

[17] Williams, Z. A., and Roux, J. A., "Graphite Foam Thermal Management of a High Packing Density Array of Power Amplifiers," *Journal of Electronic Packaging*, Vol. 128, No. 4, 2006, pp. 456–465. doi:10.1115/1.2353282

[18] Williams, Z. A., and Roux, J. A., "Thermal Management of a High Packing Density Array of Power Amplifiers Using Liquid Cooling," *Journal of Electronic Packaging*, Vol. 129, No. 4, 2007, pp. 488–495. doi:10.1115/1.2804100

[19] Williams, Z. A., and Roux, J. A., "Foam, Fin, and Nanoparticle Thermal Management of a High Density Array of Power Amplifiers Using Liquid Cooling," *Journal of Thermophysics and Heat Transfer*, Vol. 23, No. 1, 2009, pp. 162–169. doi:10.2514/1.39497

[20] Klett, J., and Conway, B., "Thermal Management Solutions Utilizing High Thermal Conductivity Graphite Foams," *Proceedings of the 45th International SAMPE Symposium and Exhibition*, Society for the Advancement of Material and Process Engineering, Covina, CA, 2000.

[21] Coursey, J. S., Kim, J., and Boudreaux, P. J., "Performance of Graphite Foam Evaporator for use in Thermal Management," *Journal of Electronic Packaging*, Vol. 127, No. 2, 2005, pp. 127–134. doi:10.1115/1.1871193